Ionization of a lithium ion by electron impact in a strong laser field

S. Ghosh Deb,[1] A. Chattopadhyay,[2] and C. Sinha[1,*]

[1]*Department of Theoretical Physics, Indian Association for the Cultivation of Science, Kolkata 700032, India*

[2]*Photon Science Institute, School of Physics and Astronomy, University of Manchester, Manchester M13 9PL, United Kingdom*

(Received 6 April 2011; revised manuscript received 2 November 2011; published 2 December 2011)

The modification in the dynamics of the electron-impact ionization process of a Li^+ ion due to an intense linearly polarized monochromatic laser field ($n\gamma e$,2e) is studied theoretically using coplanar geometry. Significant laser modifications are noted due to multiphoton effects both in the shape and magnitude of the triple-differential cross sections (TDCSs) with respect to the field-free (FF) situation. The net effect of the laser field is to suppress the FF cross sections in the zeroth-order approximation [Coulomb-Volkov (CV)] of the ejected electron wave function, while in the first order [modified Coulomb-Volkov (MCV)], the TDCSs are found to be enhanced or suppressed depending on the kinematics of the process. The strong FF recoil dominance for the (e,2e) process of an ionic target at low incident energy is destroyed in the presence of the laser field. The FF binary-to-recoil ratio changes remarkably in the presence of the laser field, particularly at low incident energies. The difference between the multiphoton CV and the FF results indicates that for the ionic target, the Kroll-Watson sum rule does not hold well at the present energy range in contrast to the neutral atom (He) case. The TDCSs are found to be quite sensitive with respect to the initial phase of the laser field, particularly at higher incident energies. A significant qualitative difference is noted in the multiphoton ejected energy distribution (double-differential cross sections) between the CV and the MCV models. Variation of the TDCSs with respect to the laser phase is also studied.

DOI: 10.1103/PhysRevA.84.063404 PACS number(s): 32.80.Wr, 34.80.Qb, 34.50.Rk

I. INTRODUCTION

Laser-assisted ionization of positive ions by charged particles (e.g., electrons, positrons) plays a very prominent role in many practical fields, such as plasma confinement in fusion plasma, laser heating of plasma, high power gas lasers, etc. Particularly, such collision processes are highly needed in the study of laser-produced plasma. Moreover, studies of such highly ionized systems present in the solar atmosphere and hot stars are extremely useful for astrophysical investigation.

For ionization of helium and its isoelectronic ions, unlike the single-electron hydrogenic ions, further complication arises in the dynamics because of the presence of two bound electrons, and effectively the problem turns to a four-body one in the final channel. Theoretically, it becomes a difficult task to frame the model of the problem and one has to resort to some approximations. Apart from the direct ionization of an electron from the ionic target, there could also be important indirect processes [1,2] that would contribute to the single ionization of the ion, e.g., excitation of an inner-shell electron with subsequent autoionization, nonradiative resonant capture of the incident electron by the ion with simultaneous excitation of the ionic core followed by deexcitation of the intermediate triply excited state by emission of two correlated electrons [1]. The latter process could give rise to resonances in the (e,2e) process of a Li^+ ion that occur when the energy available in the collision matches the intrinsic energies of the ion [1–3] and such resonances were already observed experimentally [1]. However, since such resonances are associated with multistep processes, their probability is supposed to be small. However, the total single ionization from the ionic target should include contributions from the direct as well as from the indirect channels.

In addition to the dynamics, another difficulty arises due to the inaccuracies of the approximate bound-state wave function of a helium atom or a heliumlike ion in the initial channel.

Regarding the experimental situation for the FF (e,2e) process of the Li^+ ion, the experimental works were so far limited to total or singly differential cross sections only [1–7]; no fully differential cross section [triple-differential cross section (TDCS)] measurement is yet available in the literature.

As for the theoretical situation, very few TDCS calculations exist in the literature for the (e,2e) process of Li^+ [8–13]. Unlike other authors [8–12], Mathur *et al.* [13] made a comparative study of the ionization cross sections of different ions, e.g., Li^+, Na^+, K^+, Rb^+, Cs^+, Ne^+, N^+, and Mg^+ using different velocity distribution functions for the atomic electrons, and the obtained results were discussed in light of different available theoretical and experimental results.

Nowadays in most of the experimental arrangements external laser fields are required for different purposes, e.g., collimation of the beams, cooling and trapping of particles, alignment of ions, etc. It is therefore quite worthwhile to study theoretically the modifications of the FF (e,2e) process of the ionic target (Li^+) in the presence of an external laser field, particularly in the absence of any corresponding experimental data.

As for the laser-assisted (e,2e) measurements, the first kinematically complete (TDCS) experiment was performed by Hörr *et al.* [14] for single ionization of a helium atom. This measurement indicates a bright future for the study of such a laser-assisted ionization process. However, for the ionic target, even for the simplest He^+ ion, no laser-assisted experiment is yet available in the literature, probably due to some technical problems in the measurement with ionic targets. The absence of any experimental data adds further importance to the theoretical study of such a process.

The present study addresses the multiphoton effects on the TDCS for the (e,2e) process of the ground-state Li^+ in

*chand_sin@hotmail.com

a coplanar geometry. Only the direct ionization process is considered in the present work. The effect of multiphotons on the TDCSs as well as on the double-differential cross sections (DDCSs) were already studied both experimentally [14] and theoretically [15,16] for the laser-assisted (e,2e) process of a neutral He atom where significant modifications (e.g., enhancement of the TDCS binary peak) were noted [14,16] due to multiphotonic effects when compared to the field-free (FF) cases. It will now be quite worthwhile and interesting to study the laser-assisted (e,2e) process of a He-like ion (e.g., Li^+) in order to see the effect of the long-range Coulomb interaction that occurs in the initial channel in the case of an ionic target. The main objective of the present study is to compare the TDCS of the two-electron ion Li^+ with the corresponding laser-assisted TDCS of the neutral He atom [14–16].

The laser field is chosen to be spatially homogeneous and linearly polarized represented by the vector potential $\vec{A}(t) = \vec{A}_0 \cos(\omega t + \delta)$, where $A_0 = c\varepsilon_0/\omega$, with ε_0 and ω being the field amplitude and frequency, respectively; c is the velocity of light and δ is the initial phase of the laser field. The study of TDCSs as is done in the present study provides the most detailed information for this (e,2e) process.

The interaction between the projectile electron (e) and the screened target ion (Li^+) is considered to be the perturbation responsible for the collision, while the role of the external laser is to modify the projectile electron state (Volkov wave function) as well as the initial (Li^+) and final (Li^{2+}) bound states of the target ion.

The present model takes proper account of the long-range Coulomb attraction occurring in the initial as well as in the final channels between the incident electron and the screened target ions in the framework of the Coulomb-Born approximation.

The dressed ejected electron in the combined field of the laser as well as the Coulomb field of the residual target nucleus is chosen to be a Coulomb-Volkov (CV) or a more refined wave function, the modified Coulomb-Volkov (MCV) wave function [16–19].

The dressed wave function of the Li^+ ion and the residual Li^{2+} ion are constructed in the framework of the first-order time-dependent perturbation theory, taking proper account of the orthogonality as well as the exchange effect for the two-electron wave function (Li^+).

II. THEORY

The following laser-assisted (LA) multiphoton ionization process of lithium ion (Li^+) in its ground state is studied for the exchange of n photons:

$$\begin{aligned} &Li^+(1s) + e^-(E_i,\vec{k}_i) + n\gamma(\omega,\vec{\varepsilon}_0) \\ &\quad \rightarrow e^-(E_1,\vec{k}_1) + e^-(E_2,\vec{k}_2) + Li^{2+}(1s), \end{aligned} \tag{1}$$

where E_i, E_1, E_2 and $\vec{k}_i, \vec{k}_1, \vec{k}_2$ are the energy and the momentum of the projectile, scattered and the ejected

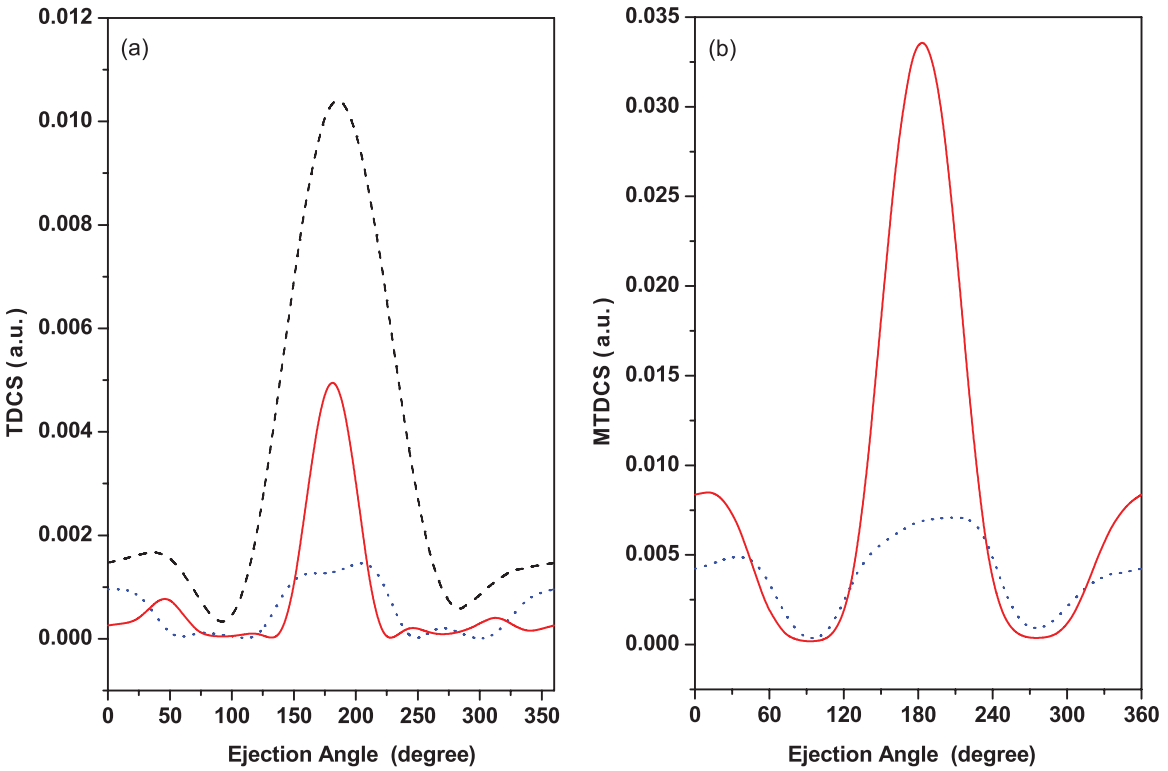

FIG. 1. (Color online) (a) Single-photon TDCS (in a.u.) for the ionization of the Li^+ ion from the ground state by electron impact, for the case $E_i = 150$ eV, $E_2 = 5$ eV, and $\theta_1 = 4^\circ$, as a function of the ejection angle (θ_2). Dashed curve: FF results; dotted curve: CV results; and solid curve: MCV results. (b) Multiphoton TDCS (MTDCS) for the same parameters as in (a).

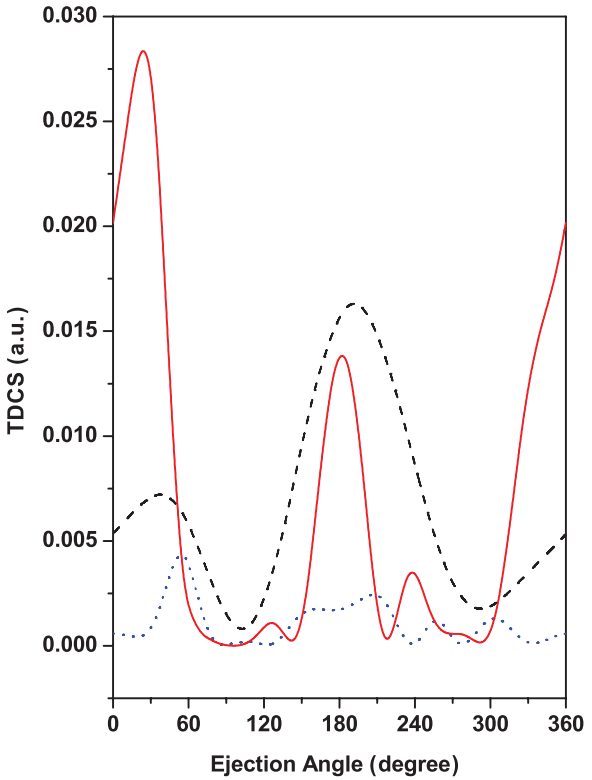

FIG. 2. (Color online) Single-photon TDCS for $E_i = 250$ eV, $E_2 = 10$ eV, and $\theta_1 = 4^\circ$; symbols are the same as in Fig. 1(a).

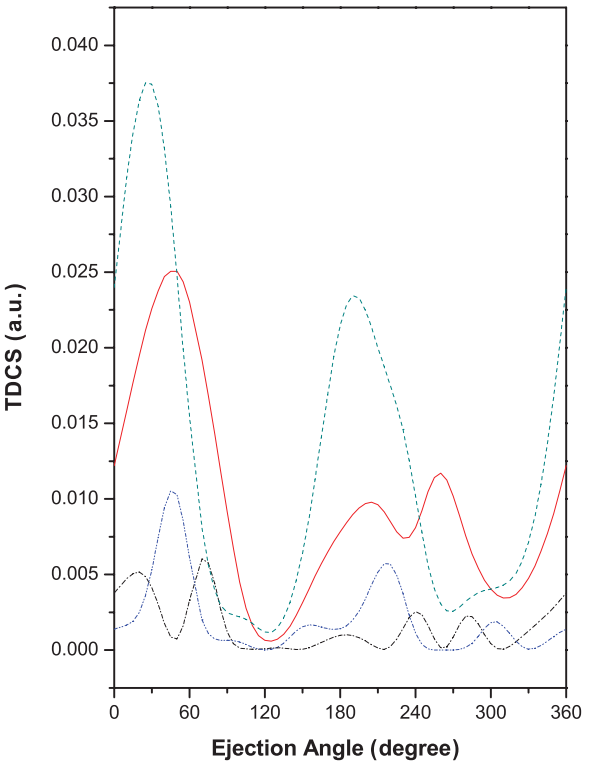

FIG. 3. (Color online) Single- and multiphoton TDCSs of Li^+ for $E_i = 500$ eV, $E_2 = 10$ eV, and $\theta_1 = 4^\circ$ in the CV and MCV models. Solid: multiphoton CV; dashed: multiphoton MCV; dashed-dotted: single-photon CV; dashed-double dotted: single-photon MCV. All the MCV cross sections are scaled down by a factor of 5 in order to place the CV and MCV in the same scale.

electron, respectively, $\gamma(\omega, \vec{\varepsilon}_0)$ represents the laser photon with frequency ω and field strength $\vec{\varepsilon}_0$.

The collision dynamics is treated quantum mechanically while the laser field is treated classically, which is quite justified for an intense laser field.

The prior form of the transition matrix element for the process (1) is given as

$$T_{if} = -i \int_{-\infty}^{\infty} dt \langle \Psi_f^- | V_i | \psi_i \rangle, \tag{2}$$

where V_i is the perturbation potential in the initial channel given by

$$V_i = -\frac{2}{r_1} + \frac{1}{r_{12}} + \frac{1}{r_{13}}, \tag{3}$$

where $\vec{r}_1$, $\vec{r}_2$, and $\vec{r}_3$ are the position vectors of the projectile electron and the two target electrons (2,3), respectively, $\vec{r}_{12} = \vec{r}_1 - \vec{r}_2$ and $\vec{r}_{13} = \vec{r}_1 - \vec{r}_3$, and ψ_i is the asymptotic initial-state wave function. The final-state wave function Ψ_f^- in Eq. (3) represents the exact solution of the Schrödinger equation

$$(H - E)\Psi_f^- = 0, \tag{4}$$

satisfying the incoming wave boundary condition. It is evident from Eq. (3) that the perturbation V_i vanishes asymptotically for $r_1 \to \infty, r_2, r_3$ finite.

In the present work the projectile-laser interaction is treated to all orders while the laser-target interaction is considered in the framework of the first-order time-dependent perturbation theory.

The initial channel asymptotic wave function ψ_i in Eq. (2) is chosen as $\psi_i = \varphi_i^d \xi_{k_i}$, where ϕ_i^d represents the dressed wave function of the ground-state Li^+ ion [20,21]:

$$\phi_i^d(r_2, r_3, t) = \exp(-i W_0 t) \exp(-i \vec{a} \cdot \vec{R}) \times \left[\phi_0(\vec{r}_2, \vec{r}_3) - \sin \omega t \sum_{n'} \frac{\omega_{n'0} M_{n'0}}{(\omega_{n'0}^2 - \omega^2)} \phi_{n'}(\vec{r}_2, \vec{r}_3) - i \cos \omega t \sum_{n'} \frac{\omega M_{n'0}}{(\omega_{n'0}^2 - \omega^2)} \phi_{n'}(\vec{r}_2, r_3) \right], \tag{5}$$

where $\vec{R} = \sum_{j=1'}^{2} \vec{r}_j$ is the sum of the target coordinates, $\omega_{n'0} = W_{n'} - W_0$ is the atomic excitation frequency, W_0 is the ground-state energy, $M_{n'0} = \vec{\varepsilon}_0 \cdot \langle \phi_{n'} | \vec{R} | \phi_0 \rangle$, and $\phi_0(\vec{r}_2, \vec{r}_3)$ is the unperturbed ground-state wave function of Li^+ and is given by

$$\phi_i(\vec{r}_2, \vec{r}_3) = u(\vec{r}_2) u(\vec{r}_3) = \frac{\lambda_i^3}{\pi} e^{-\lambda_i (\vec{r}_2 + \vec{r}_3)}, \tag{6}$$

where $\lambda_i = (Z - 1) + 0.6875$ is the effective charge of the target nucleus, $Z(=3)$ being the actual target nucleus charge. The factor $e^{-i\vec{a}\cdot\vec{R}}$ in Eq. (5) ensures the gauge consistency between the dressed projectile wave function in the Coulomb gauge (to be described below) and the dressed target wave function (in the electric-field gauge) [19], with $\vec{a} = \vec{\varepsilon}_0/\omega$.

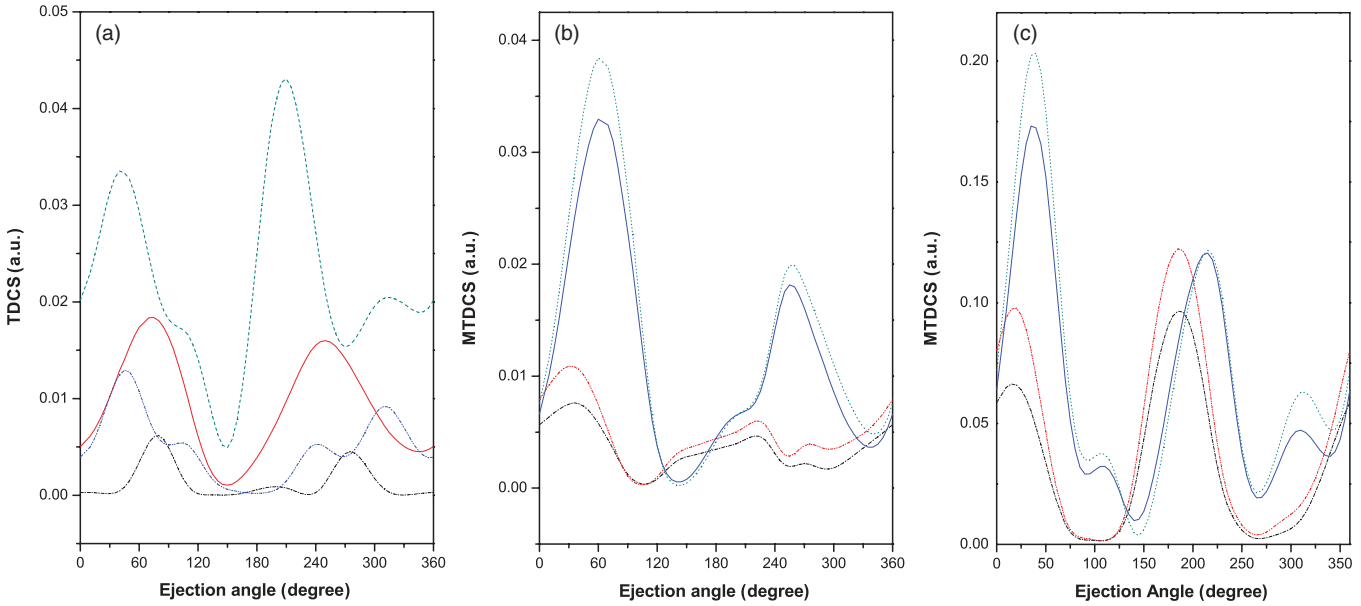

FIG. 4. (Color online) (a) Same as in Fig. 3 but for $E_i = 1000$ eV, $E_2 = 3$ eV, and $\theta_1 = 6^0$, without any scaling factor. (b) Multiphoton TDCS (MTDCS) with and without the final-state correlation term in Eq. (12) for the CV model for the parameters $E_i = 1000$ eV and $E_i = 250$ eV, $E_2 = 10$ eV and $\theta_1 = 4^\circ$. Solid: 1000 eV with correlation (CR); dotted: 1000 eV without correlation (WCR); dashed-dotted: 250 eV (CR); dashed-double-dotted: 250 eV (WCR). (c) Same as in (b) but for the MCV model.

The dressed ground-state wave function for the target Li^+ ion $\Phi_i^d(\vec{r}_2,\vec{r}_3,t)$ satisfies the following time-dependent Schrödinger equation (in the electric-field gauge),

$$[H_0 + V(t)]\,\Phi_i^d(\vec{r}_2,\vec{r}_3,t) = i\frac{\partial}{\partial t}\Phi_i^d(\vec{r}_2,\vec{r}_3,t), \tag{7}$$

where H_0, the unperturbed Hamiltonian for the target ion, and the perturbation $V(t)$ are given by $H_0 = -(1/2)\nabla_2^2 - (1/2)\nabla_3^2 - (Z/r_2) - (Z/r_3) + (1/|\vec{r}_2 - \vec{r}_3|)$; $V(t) = \vec{\varepsilon}(t)\cdot(\vec{r}_2 + \vec{r}_3)$.

The time dependence of $\Phi_i^d(\vec{r}_2,\vec{r}_3,t)$ is assumed to be in the form

$$\Phi_i^d(\vec{r}_2,\vec{r}_3,t) = \psi\,\exp\left[-i\int E^{(1)}(t)dt\right], \tag{8}$$

where $E^{(1)}$ is the energy corrected up to first order and ψ is the first-order solution of the following Schrödinger equation for a heliumlike ion in a uniform electric field

$$\frac{1}{2}\nabla_2^2\psi + \frac{1}{2}\nabla_3^2\psi + \left(E + \frac{Z}{r_2} + \frac{Z}{r_3} - \frac{1}{r_2 r_3}\right) = \varepsilon z\psi, \tag{9}$$

where $\vec{\varepsilon}$ is the external field in the direction of the z axis. If the frequency of the applied field is sufficiently low (soft photon limit), its effect can be treated quasistatically. In view of the closure approximation [22,23] and the fact that $\omega \ll \omega_{n'0}$ (in the soft photon limit), with the help of Eqs. (7)–(9), Eq. (5) can be written as

$$\phi_i^d(r_2,r_3,t) = \exp(-iW_0 t)\exp(-i\vec{a}\cdot\vec{R})\left[\phi_0(\vec{r}_2,\vec{r}_3) - \sin\omega t\frac{\vec{\varepsilon}_0\cdot\vec{R}}{\bar{\omega}+\omega}\phi_0(\vec{r}_2,\vec{r}_3)\right]. \tag{10}$$

$\bar{\omega} = W_n - W_0$ is the average excitation energy of the Li^+ atom and is chosen to be 0.90 a.u. [24].

The dressed wave function of the incident electron (ξ_{k_i}) in the combined field of the laser and the screened target ion is considered to be of CV type [25], due to the long-range Coulomb attraction as given below, while for the neutral target, it was a plane-wave Volkov wave function. Thus the dressed incident electron wave function in presence of the laser field is given by

$$\xi_{k_i}(\vec{r}_1) = \exp\left\{-i\left[k_i\cdot r_1 - k_i\cdot\alpha_0\,\sin(\omega t+\delta) - E_{k_i}t\right]\right\} \times C_i\,{}_1F_1[-i\alpha_i,1,-i(k_i r_1 - \vec{k}_i\cdot\vec{r}_1)], \tag{11}$$

where $C_i = \exp(\pi\alpha_i/2)\Gamma(1+i\alpha_i)$ is the Coulomb normalization constant with $\alpha_i = (Z-2)/k_i$, $Z(=3)$ being the charge of the target ion.

In order to construct the wave function (Ψ_f^-) for the final channel which involves four particles, we adopt the following assumption. We have reduced the four-body problem to a three-body one in the sense that the bound passive electron plays no other role than to screen the nucleus from the two outgoing particles. For the single ionization this assumption is expected to be quite reasonable, particularly for fast electron impact. The final channel wave function Ψ_f^- in Eq. (2) satisfying the exact asymptotic three-body incoming wave boundary condition for the ionization process is approximated as

$$\Psi_f^- = \chi_f^d(\vec{r}_3)\xi_{k_j}(\vec{r}_j)C_{12}\,{}_1F_1[-i\alpha_{12},1,-i(k_{12}r_{12}+\vec{k}_{12}\cdot\vec{r}_{12})], \tag{12}$$

where $\chi_f^d(\vec{r}_3)$ represents the dressed wave function of the residual target nucleus (Li^{2+}); ξ_{k_j} $(j = 1,2)$ refers to the scattered or the ejected electron wave function in the final channel. The last term in Eq. (12) containing the confluent

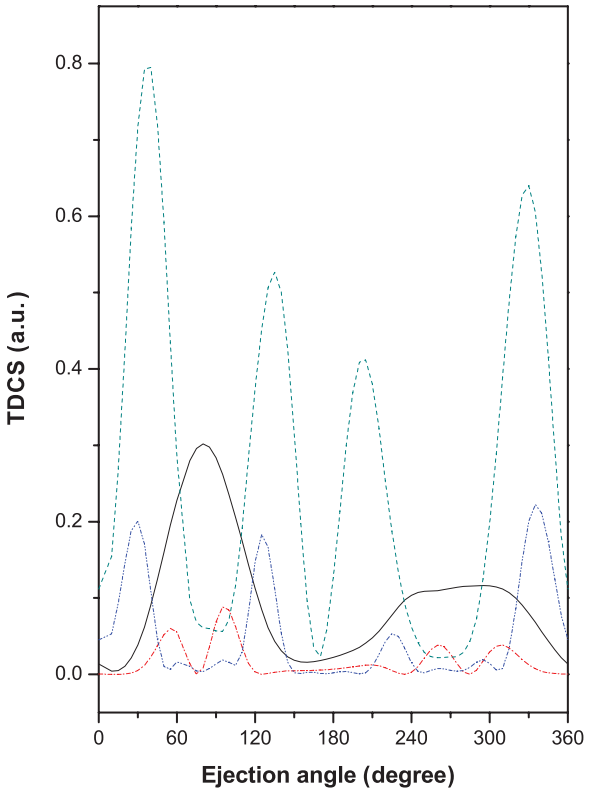

FIG. 5. (Color online) Single- and multiphoton TDCSs of a He atom for $E_i = 500$ eV. $E_2 = 10$ eV and $\theta_1 = 4^\circ$ in the CV and MCV models. Solid: multiphoton CV; dashed: multiphoton MCV; dashed-dotted: single-photon CV; dashed-double dotted: single-photon MCV. All the MCV cross sections are scaled down by a factor of 5 in order to place the CV and MCV in the same scale.

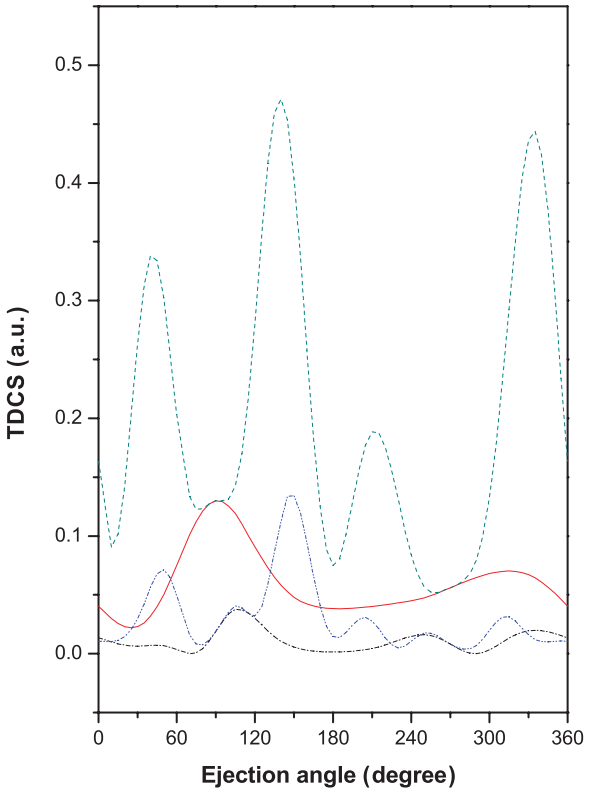

FIG. 6. (Color online) Same as in Fig. 5 for a He atom but for the parameters $E_i = 1000$ eV, $E_2 = 3$ eV, and $\theta_1 = 6^\circ$, without any scaling factor.

hypergeometric function represents the Coulomb correlation [25,26] between the scattered ($\vec{r}_1$) and the ejected ($\vec{r}_2$) electrons in the final channel with $\alpha_{12} = 1/2|\vec{k}_{12}|$, $\vec{k}_{12} = \frac{1}{2}(\vec{k}_1 - \vec{k}_2)$, and $C_{12} = \exp(\pi\alpha_{12}/2)\,\Gamma(1 + i\alpha_{12})$ is the Coulomb normalization constant.

Now, the scattered electron wave function ξ_{k_1} satisfies the equation

$$i\frac{\partial}{\partial t}\xi_{k_1}(\vec{r}_1,t) = \left[\frac{p^2}{2} + \frac{1}{c}\vec{A}\cdot\vec{p} - \frac{Z_{\rm sc}}{r}\right]\xi_{k_1}(\vec{r}_1,t) \qquad (13)$$

and is described by the Coulomb-Volkov wave function given by

$$\xi_{k1}(\vec{r}_1,t) = (2\pi)^{-3/2}\exp\left\{i[\vec{k}_1\cdot\vec{r}_1 - \vec{k}_1\cdot\vec{\alpha}_0\,\sin(\omega t+\delta) - E_{k_1}t] - i/2c^2\int_{-\infty}^{t}A^2(t')dt'\right\} \times C_{1\,1}F_1[-i\alpha_1,1,-i(k_1r_1+\vec{k}_1\cdot\vec{r}_1)], \qquad (14)$$

where $\alpha_1 = Z_{\rm sc}/k_1$, $Z_{\rm sc} = Z - 1$, being the screened charge of the target atom as seen by the scattered electron.

The ejected electron wave function χ_f^d with momentum $\vec{k}_2$ in the combined field of the residual target nucleus (Li^{2+}) and the external laser field is first proposed by Joachain *et al.* [18,19] with necessary changes for the Li^+ ion (i.e., with $\alpha_2 = Z_{\rm sc}/k_2$) and is given by

$$\chi_f^d(\vec{r}_2,t) = \exp\left(-iE_{k_2}t\right)\exp(-i\vec{a}\cdot\vec{r}_2)\exp[i\vec{k}_2\cdot\vec{\alpha}_0\sin(\omega t+\delta)] \times\left\{\psi_{c,k_2}^{(-)}(\vec{r}_2) + \frac{i}{2}\sum_n\left[\frac{\exp[i(\omega t+\delta)]}{E_n - E_{k_2}+\omega} - \frac{\exp[-i(\omega t+\delta)]}{E_n - E_{k_2}-\omega}\right] \times M_{nk_2}\psi_n(\vec{r}_2) + i\vec{k}_2\cdot\vec{\alpha}_0\,\sin(\omega t+\delta)\psi_{c,k_2}^{(-)}(\vec{r}_2)\right\}, \qquad (15)$$

where $\psi_{c,k_2}^{(-)}(\vec{r}_2) = (2\pi)^{-3/2}C_2\exp(i\vec{k}_2\cdot\vec{r}_2)_1F_1[-i\alpha_2,1, -i(k_2r_2+\vec{k}_2\cdot\vec{r}_2)]$; $\alpha_2 = Z/k_2$; E_{k_2} being the energy of the ejected electron and the Coulomb normalization constant $C_j = \exp(\pi\alpha_j/2)\Gamma(1+i\alpha_j)$ and $M_{n,k_2} = \langle\psi_n|\,\vec{\varepsilon}_0\cdot\vec{r}_2|\psi_{c,k_2}^{(-)}\rangle$.

The main difficulty lying with the evaluation of Eq. (15) is to perform the infinite summation running over the whole atomic spectrum. To circumvent this problem, some mathematical techniques were adopted for laser-assisted inelastic collisions with neutral targets, e.g., the Coulomb Green's function [19] for proper evaluation of the infinite summation or a fully nonperturbative Floquet technique while the use of closure approximation [22] was questioned by Martin *et al.* [19], particularly for the case of continuum states. However, for the ionic target, even the field-free ionization problem is quite difficult to solve rigorously because of the presence of the long-range Coulomb interaction between the projectile and the target. As such, as a first attempt, we resort to closure

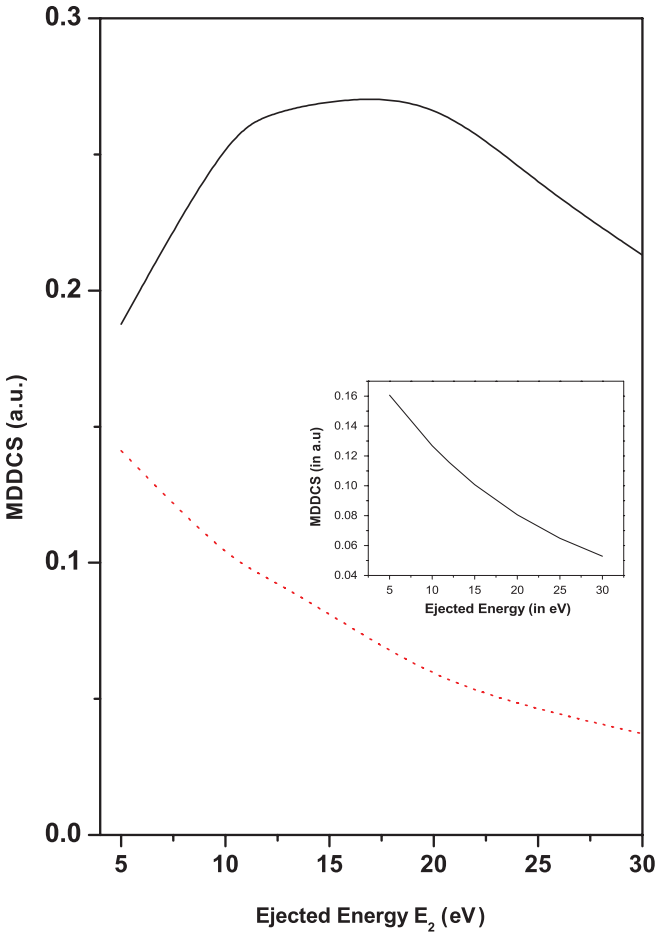

FIG. 7. (Color online) Multiphoton doubly differential cross section (MDDCS) for $\sum\theta_2,\phi_2$ (in a.u.) as a function of the ejected energy (E_2) at an incident energy $E_i = 250$ eV, $\theta_1 = 3^\circ$. Solid curve: MCV results; dotted curve: CV results scaled up by a factor of 2. Inset: Field-free (FF).

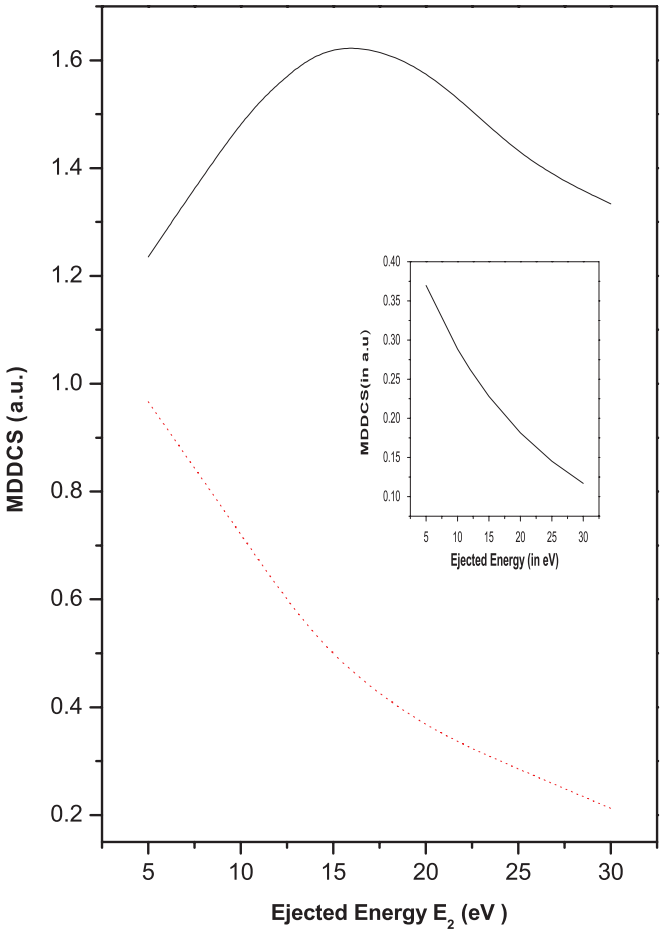

FIG. 8. (Color online) Same multiphoton DDCS but for incident energy $E_i = 1000$ eV, $\theta_1 = 1.5^\circ$; CV is scaled by a factor of 3.

approximation [22] for the evaluation of the infinite summation occurring in Eq. (15), the average excitation energy $\bar{E}_n$ being chosen to be the ionization energy of target Li^{2+}. As for some justification of the use of closure approximation, it may be pointed out that for $E_n \gg E_{k_2} \pm \omega$ (as happens to be the case in the present work), the contribution of the term containing the infinite summation is negligible as compared to the other two terms in Eq. (15). Further, we have also tested the sensitivity of our calculation by varying the average excitation energy ($\bar{E}_n$) around its expected value. The results are found to be quite insensitive with respect to the choice of $\bar{E}_n$, which also extends support to the reliability of the present calculation.

It may be noted that the first term of Eq. (15), the zeroth-order result, is reduced to the CV solution as described in Eq. (11), while the full continuum dressing term in Eq. (15) refers to the MCV solution.

In deriving the ejected electron wave function (15), we have neglected the contributions to the electron states arising from $A^2/2c^2$ terms. For the present kinematics the ponderomotive potential energy is much smaller than the frequency of the laser field so that the neglect is quite legitimate.

To account for the orthogonality in the case of the two-electron wave function, we can write the final channel (correlated three-body) wave function Ψ_f^- in the following form:

$$\Psi_f^- = \zeta_{k_j}(\vec{r}_1)\exp(\pi\alpha_{12}/2)\Gamma(1+i\alpha_{12})_1F_1 \times [-i\alpha_{12},1;-i(k_1r_{12}+\vec{k}_1\cdot\vec{r}_{12})]\bar{\Phi}(\vec{r}_2,\vec{r}_3). \quad (16)$$

The wave function $\bar{\Phi}(\vec{r}_2,\vec{r}_3)$ in Eq. (16) of the two-electron atom subsystem in the final channel is represented by a symmetrized product of the one-electron ion (Li^{2+}) ground-state wave function (χ_f^d) for the bound electron ($\vec{r}_3$) with the dressed continuum wave function ($\bar{\xi}_{k_2}$) for the ejected electron with momentum $\vec{k}_2$ [orthogonalized to the ground-state orbital $u(\vec{r})$]. Thus,

$$\bar{\Phi}(\vec{r}_2,r_3)\frac{1}{\sqrt{2}}\left[\bar{\xi}_{k_2}(\vec{r}_2)\chi_f^d(\vec{r}_3)+\bar{\xi}_{k_2}(\vec{r}_3)\chi_f^d(\vec{r}_2)\right], \quad (17)$$

with $\bar{\xi}_{k_2}(\vec{r}) = \xi_{k_2}(\vec{r}) - \langle u|\xi_{k_2}\rangle u(\vec{r})$, where $u(\vec{r})$ corresponds to the ground-state orbital.

It should be noted here that in calculating the matrix element corresponding to the second term (i.e., the exchange term) in Eq. (17) we have replaced the coordinates "2" and "3" in the remaining part of the expression Ψ_f^- in Eq. (16) for the sake of consistency.

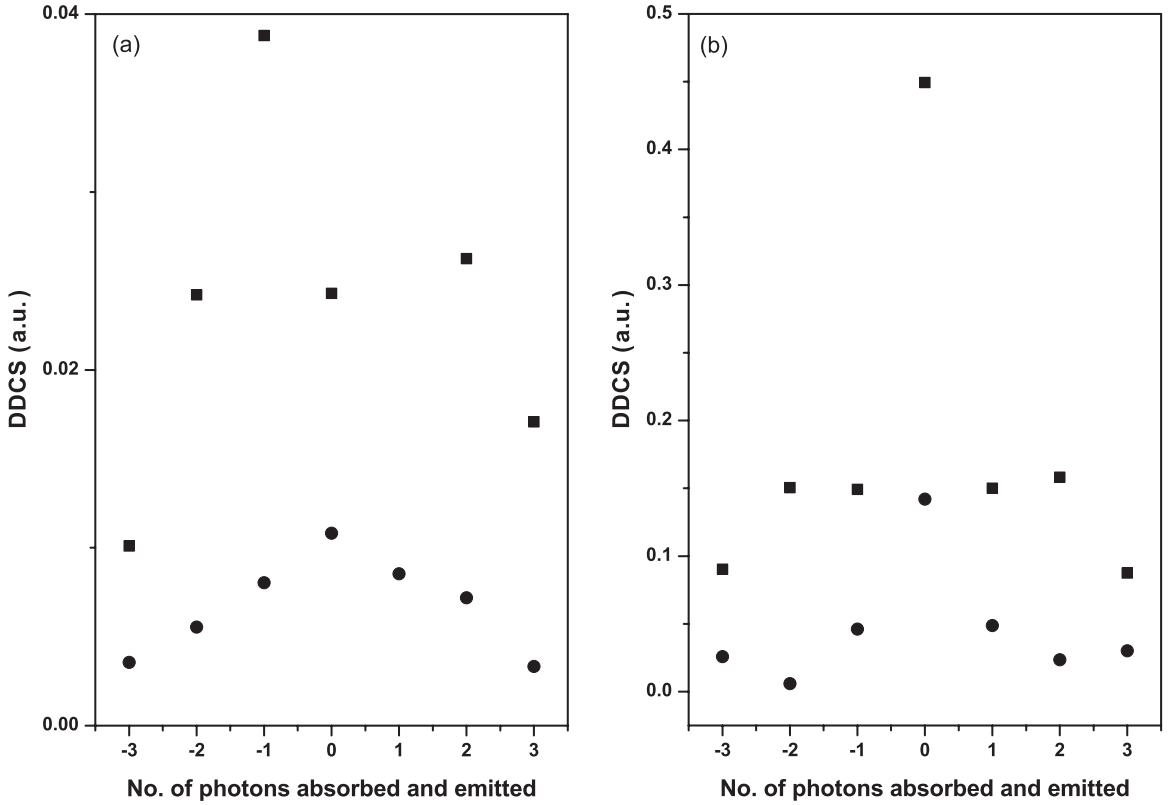

FIG. 9. Double-differential cross sections as a function of individual photon distributions at energies (a) $E_i = 250$ eV and (b) $E_i = 1000$ eV.

The dressed ground-state wave function $\chi_f^d(\vec{r})$ [in Eq. (17)] of the hydrogenlike ion (e.g., Li^{2+}) is given by [25]

$$\chi_f^d(\vec{r},t) = e^{-i\vec{a}\cdot\vec{r}}\frac{1}{\sqrt{\pi}}e^{-iW_0t}e^{-\lambda_f\vec{r}}\left[1-\sin(\omega t+\delta)\times\vec{\varepsilon}_0\cdot\vec{r}\left(1+\frac{Zr}{2}\right)\right], \tag{18}$$

where λ_f is the final-state bound-state parameter of the hydrogenlike ion Li^{2+}.

Equation (2) is evaluated analytically to obtain the transition matrix element

$$T_{if}^n = -i\sum_n \delta(E_1+E_2-E_i-n\omega)J_n(\beta)I, \tag{19}$$

where $J_n(\beta)$ is the spherical Bessel function of order n [27] with

$$\beta = D(\cos\delta+\sin\delta), \tag{20}$$

with $\vec{D} = \vec{K}\cdot\vec{\alpha}_0$, where $\vec{K} = (\vec{k}_1+\vec{k}_2)-\vec{k}_i$; I stands for the space integral of T_{if} and $I = f_n - f_O$, f_n being the nonorthogonal part (corresponding to $\vec{\xi}_{k_2} = \xi_{k_2}$ in Eq. (17) and f_O the orthogonal part of the space part in the ionization amplitude.

The summation index "n" in Eq. (19) stands for the number of photon transfer and can take values $n = 0, \pm1, \pm2, \pm3, \ldots$. The zero value corresponds to no photon transfer while the upper (lower) sign corresponds to photon absorption (emission).

The expressions for the TDCSs and DDCSs accompanied for transfer of an n number of photons are, respectively, given by

$$\frac{d^3\sigma}{d\Omega_1\,d\Omega_2\,dE_2} = \frac{k_1k_2}{k_i}\left|T_{if}^n\right|^2, \tag{21}$$

$$\frac{d^2\sigma}{dE_2\,d\Omega}_{1,2} = \int\frac{d^3\sigma}{dE_2\,d\Omega_1\,d\Omega_2}d\Omega_{1,2}. \tag{22}$$

In this calculation we have neglected the electron exchange effect between the projectile and the target electron in the final channel, which could be legitimate for such a LA process [16,28].

The multiphoton cross sections MTDCS (MDDCS) denote the summation of the single-photon TDCS (DDCS) in Eqs. (21) and (22) over all possible values of n, the number of photons exchanged during the collision (including both absorption and emission). In the present work we have considered $n = \pm3$ and have noted that after that, the contribution to the aforesaid summation decreases significantly.

III. RESULTS AND DISCUSSIONS

We have computed the TDCSs as well as the DDCSs for electron impact ionization of a Li^+ ion from its ground state in the presence of a laser field for different kinematical situations at intermediate and high incident energies in the coplanar asymmetric geometry. The laser field is chosen to be parallel to the incident momentum direction. Both single and multiphoton effects are considered in the TDCS level. The photon energy

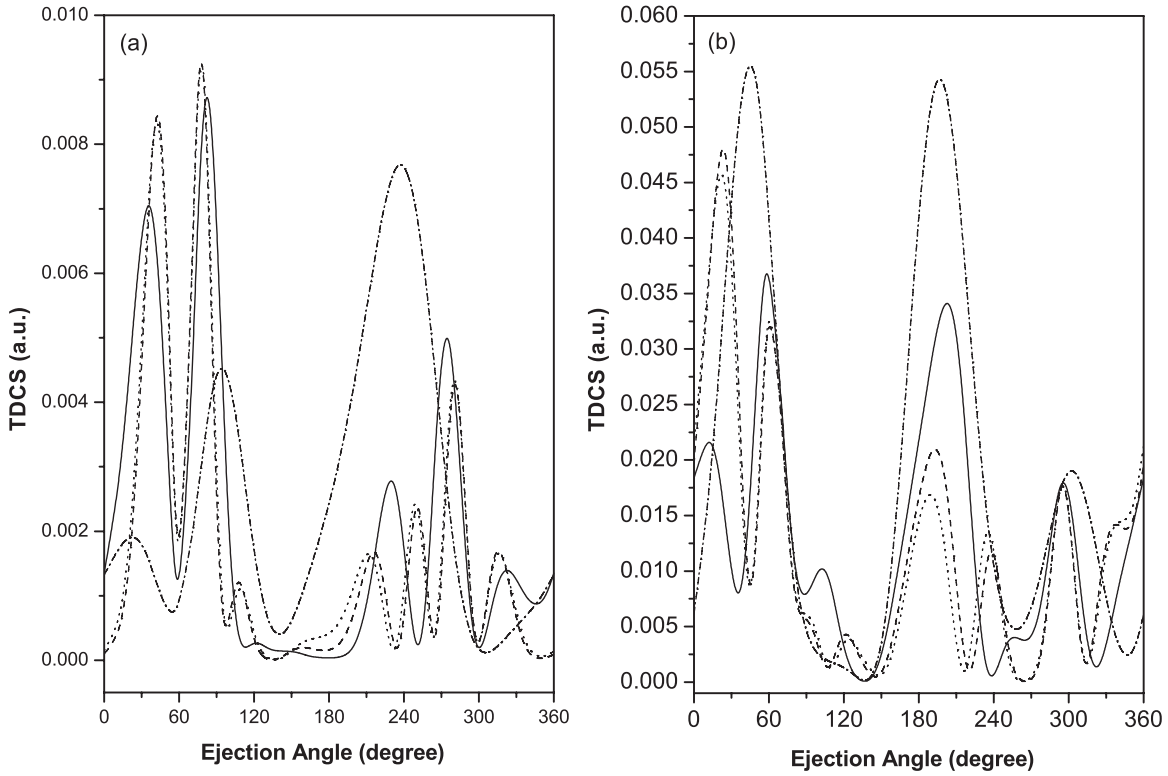

FIG. 10. Variation of TDCSs for different values of the initial phase δ of the laser field for single-photon absorption at $E_i = 1000$ eV (a) for the CV case and (b) for the MCV case. Solid curve: $\delta = 0^\circ$, 90°, and 180°; dashed curve: $\delta = 45^\circ$; dotted curve: $\delta = 60^\circ$; and dashed-dotted curve: $\delta = 120^\circ$.

(ω) and the laser field strength (ε_0) are respectively chosen as 1.17 eV and 5×10^9 V/m (Ti:sapphire laser).

Figures 1–4 display the present single photon as well as the multiphoton TDCS (MTDCS) of Li^+ against the angle of ejection of the slower electron (θ_2). We have also presented the corresponding single and multiphoton TDCS results for the neutral target He atom [15,16] in Figs. 5 and 6 for incident energies 500 (Fig. 5) and 1000 eV (Fig. 6) for comparison in order to see the effect of the initial channel long-range Coulomb interaction that particularly occurs for the ionic target (Li^+) but is absent in the case of a neutral target (He). Since no TDCS experiments have yet been performed for the Li^+ ion, both in the FF and in the LA situations, we are not in a position to compare our results with experiments.

Figure 1 exhibits the laser-assisted TDCS of the ground-state Li^+ ion along with the corresponding FF results in the asymmetric geometry with the kinematics $E_i = 150$ eV, $E_2 = 5$ eV, and $\theta_1 = 4^\circ$ for both the single-photon [Fig. 1(a)] and the multiphoton [Fig. 1(b)] exchange. A strong recoil peak, much larger than the binary one, is noted in the FF case, at this low incident energy, as is expected for an ionic target [11]. This behavior (i.e., the intense recoil peak even larger than the binary one) is a peculiarity for an ionic target at lower incident energies. Since the recoil peak is mainly governed by the electron-nucleus interaction, the large recoil peak at low incident energy may qualitatively be explained by the strong elastic scattering from the nucleus.

Regarding the laser modifications, both the single photon CV and the MCV results are strongly suppressed with respect to the FF ones in both the binary and recoil regions, the suppression being much more for the CV TDCS [vide Fig. 1(a)]. With increasing incident energy (say $E_i = 250$ eV; Fig. 2), the degree of suppression for the single-photon MCV TDCS (with respect to FF) decreases (particularly in the recoil region) and it gradually overestimates the FF at high incident energies [e.g., $E_i = 500$, 1000 eV; see Figs. 3(a) and 4(a)] while for the CV, the suppression (with respect to FF) retains with lesser extent even for higher incident energies (Figs. 3 and 4).

As for the multiphoton CV, at lower E_i [e.g., 150 eV; Fig. 1(b)], the intense recoil peak noted in the FF case at this low incident energy is strongly suppressed by the application of the laser field though maintaining the FF qualitative behavior, i.e., ratio $b/r < 1$, while the modification in binary peak due to laser is comparatively much less.

For higher E_i [e.g., 500, 1000 eV; vide Figs. 3(b) and 4(b)], the suppression in the recoil peak decreases while the LA binary peak is slightly enhanced with respect to the FF. It may be pointed out in this context that the dominance of the recoil peak (over the binary one) gradually diminishes, as in the FF situation, with increasing E_i [e.g., 150, 250 eV; see Figs. 1(b) and 4(b)] until at $E_i = 500$ eV [Fig. 3(b)], the LA binary peak overtakes the recoil one. Thus the FF recoil dominance of the (e,2e) process of Li^+ [11] is destroyed (changing the b/r ratio from <1 to >1) by the laser field except at low (e.g., 150 eV) incident energies in both the models (CV, MCV).

In order to see the effect of the final-state correlation between the scattered and the ejected electrons [vide Eq. (12)],

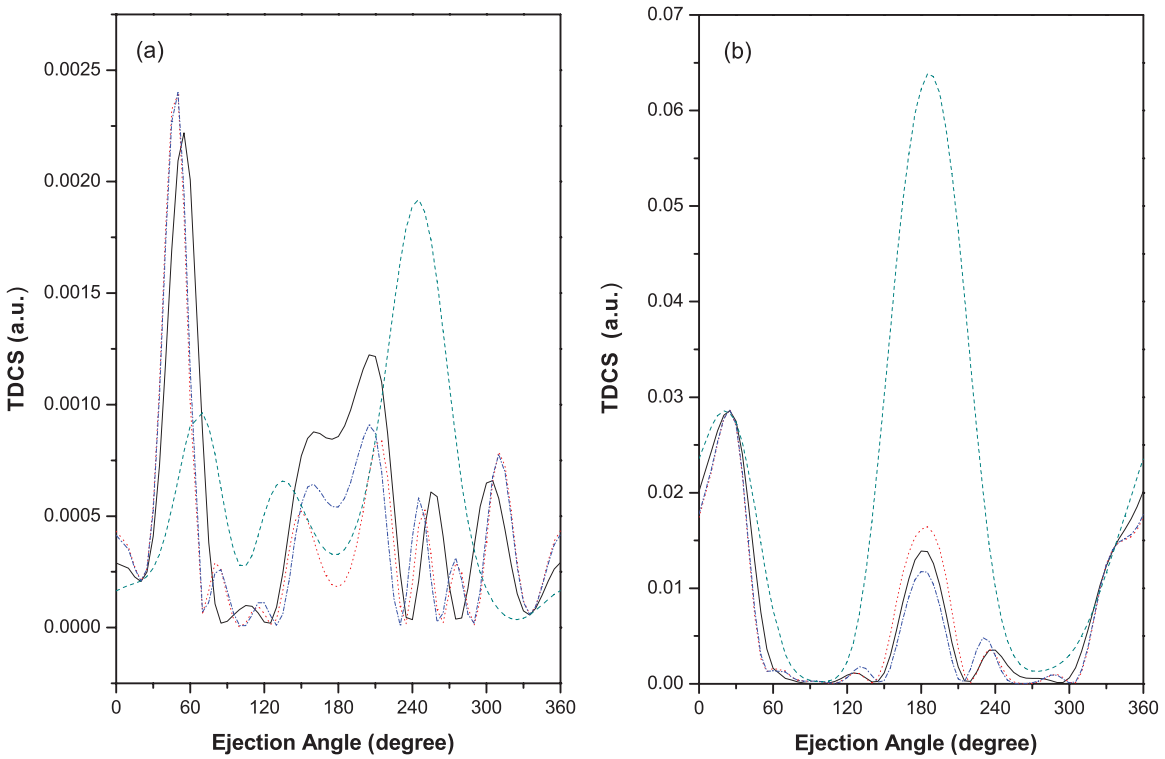

FIG. 11. (Color online) Same as in Fig. 10 but for a lower incident energy, $E_i = 250$ eV.

we have presented the multiphoton TDCS (MTDCS) results in Figs. 4(b) and 4(c) both with and without the correlation term in Eq. (12) for both the CV [Fig. 4(b)] and the MCV [Fig. 4(c)] models. As may be revealed from the figures, the effect of the final-state correlation is to reduce the cross sections to some extent in both the models. However, the qualitative behavior remains more or less the same in the two cases (with or without correlation) except for some (slight) shifting in the peak positions.

The enhancement noted in the present multiphoton binary peak at higher incident energy corroborates qualitatively the experimental findings due to Hörr *et al.* [14] for the neutral He target at high incident energy. The difference between the multiphoton CV and the FF indicates that for the ionic target (Li^+), the Kroll-Watson (KW) sum rule [25] does not hold well at the present energy range in contrast to the neutral atom case [16,29] where the KW sum rule was obeyed. The deviation from the KW sum rule (in the limit of zero target dressing) in turn reveals that the effect of target dressing in the present CV model is quite important for the ionic target.

Regarding the MCV model, the MTDCSs are enhanced remarkably with respect to the FF even at the lower incident energies indicating the importance of multiphoton effects (cf. single photon; Fig. 1 at 150 eV).

Further, the multiphoton CV recoil peaks are shifted towards higher ejection angles with respect to the FF while the binary peaks more or less maintain the FF positions. In contrast, both the MCV binary and recoil peaks are shifted towards lower ejection angles.

As for the comparison of the present TDCS (for Li^+) with the corresponding results of neutral He [16], the TDCSs for the He atom are found to be much higher (almost by an order of magnitude) than those for the Li^+ ion [vide Figs. 3, 4(a), 5, and 6] for both the CV and MCV models, indicating that the long-range Coulomb interaction in the initial channel for the latter suppresses the cross sections. Further, the b/r ratio for He (e.g., ∼1.86 in the MTDCS of Fig. 5) is much higher than that for Li^+ (∼1.32 in the MTDCS of Fig. 3) arising due to the stronger recoil peak for the ionic target (as compared to the neutral one) as discussed above in the context of Fig. 1.

Figures 7 and 8 demonstrate the energy distribution of the ejected electron at $E_i = 250$ and 1000 eV. The figures reveal that at lower E_i (e.g., 250 eV; Fig. 7), the CV multiphoton DDCS (MDDCS) falls off much more slowly as compared to the high-energy E_i (e.g., 1000 eV; Fig. 8) case where the DDCS falls off monotonically with a much higher slope (i.e., more steep). In contrast, the MCV DDCS shows a broad peaklike structure, the magnitude of the peak at higher E_i being about three times higher than that of the lower energy. The FF DDCS (vide insets of Figs. 7 and 8) indicate the modifications of the DDCS due to the laser field and reveals that the CV is somewhat lowered while the MCV is significantly enhanced with respect to the FF. The qualitative nature of the MCV curve is also changed drastically giving rise to a flat peak, unlike the monotonic fall of both the CV and the FF.

Figure 9 illustrates the individual photon (n) distributions with respect to the DDCS at $E_i = 250$ and 1000 eV and is self-explanatory.

Finally, Figs. 10 and 11 demonstrate the variation of the single-photon absorption ($l = +1$) TDCS with respect to the initial phase ($\delta = 0^\circ - 120^\circ$) of the laser field at $E_i = 1000$ (Fig. 10) and 250 eV (Fig. 11) for the CV [Figs. 10(a) and 11(a)] and the MCV cases [Figs. 10(b) and 11(b)]. The TDCS is found to be quite sensitive both qualitatively and quantitatively

with respect to the laser phase in both the models at this high incident energy. As evident from Fig. 10(a), the CV TDCS with $\delta = 45^\circ$ and 60° exhibits almost similar behavior and the binary-to-recoil peak intensity ratio is >1, as in the case of $\delta = 0^\circ$, while for $\delta = 120^\circ$, this characteristic no longer holds since in this case the binary-to-recoil ratio becomes <1 and follows the nature of the FF [11]. On the other hand, for the MCV case [Fig. 10(b)], the binary-to-recoil ratio is always >1, irrespective of the phases, although for $\delta = 0^\circ$ and 120°, the ratio is only slightly >1. It may be pointed out here that the TDCS for laser phases $\delta = 0^\circ$, 90°, and 180° coincide with each other as follows from the theory [vide Eq. (20)].

At a lower incident energy (250 eV), on the other hand, the phase variation of both the CV and the MCV TDCSs [Figs. 11(a) and 11(b)], particularly of the latter, is not very sensitive in the binary regions, while the recoil regions have some phase variations in both cases. This is quite legitimate as at lower incident energy, the collision takes place longer and phase averaging is expected to occur. The phase-averaged TDCS at this energy almost coincides with that of $\delta = 0^\circ$. The TDCSs for $\delta = 120^\circ$ exhibit some exception in both the CV and MCV cases, e.g., the b/r ratio is $\ll 1$ (i.e., follows the FF behavior), unlike the other phases where b/r is >1.

IV. CONCLUSIONS

The salient features of the present study can be outlined as follows.In the zeroth-order dressing of the ejected electron (CV), the laser modification on the TDCS is much more effective in the recoil region than in the binary, while in the first-order dressing (MCV), both the binary and the recoil peaks are modified significantly.

A large discrepancy is noted between the CV and MCV results. The overall effect of the laser field is to suppress the CV cross sections, while modification in the MCV is highly sensitive to the kinematics of the process.

The strong FF recoil dominance for $(e,2e)$ of an ionic target is not retained in the presence of the laser field. The FF b/r ratio is modified significantly at low incident energies by the laser field.

The effect of the final-state e-e correlation is to reduce the magnitude of the cross sections in both the CV and MCV models, while the qualitative behavior does not change significantly.

The laser modification decreases with increasing incident energy, as is expected physically.

The deviation of the multiphoton CV from the FF results (thereby violating the Kroll-Watson sum rule) reveals the importance of the target dressing for ionic targets, unlike the neutral target (H or He atom) where the KW sum rule was found to be valid.

The cross sections are found to be quite sensitive with respect to the laser phase, particularly at higher incident energies, while at lower energies, phase averaging might take place.

[1] A. Muller, G. Hofmann, B. Weissbecker, M. Stenke, K. Tinschert, M. Wagner, and E. Salzborn, Phys. Rev. Lett. **63**, 758 (1989).
[2] G. Hoffmann, A. Muller, K. Tinschert, and E. Salzborn, Z. Phys. D **16**, 113 (1990).
[3] Alfred Muller, J. Phys.: Conf. Series **194**, 012002 (2009).
[4] J. B. Wareing and K. J. Dolder, Proc. Phys. Soc. London **91**, 887 (1967).
[5] B. Peart and K. T. Dolder, J. Phys. B **1**, 872 (1968).
[6] W. C. Lineberger and J. W. Hooper, Phys. Rev. **141**, 151 (1966).
[7] A. Borovik Jr., A. Müller, S. Schippers, I. Bray, and D. V. Fursa, J. Phys. B: At. Mol. Opt. Phys. **42**, 025203 (2009).
[8] A. Roy, K. Roy, and N. C. Sil, Phys. Lett. A **95**, 63 (1983).
[9] R. Biswas and C. Sinha, J. Phys. B **28**, 1311 (1995).
[10] Y. Khajuria and D. N. Tripathi, Phys. Rev. A **59**, 1197 (1999).
[11] B. Nath and C. Sinha, Phys. Rev. A **62**, 052713 (2000).
[12] M. K. Srivastava, Pramana, J. Phys. **63**, 1053 (2004).
[13] K. C. Mathur, A. N. Tripathi, and S. K. Joshi, Phys. Rev. **184**, 242 (1969).
[14] C. Höhr, A. Dorn, B. Najjari, D. Fischer, C. D. Schröter, and J. Ullrich, Phys Rev. Lett. **94**, 153201 (2005).
[15] S. Ghosh Deb and C. Sinha, J. Phys.: Conf. Series **185**, 012011 (2009).
[16] S. Ghosh Deb and C. Sinha, Eur. Phys. J. D **60**, 287 (2010).
[17] D. M. Volkov, Z. Phys. **94**, 250 (1935).
[18] C. J. Joachain, P. Francken, A. Maquet, P. Martin, and V. Veniard, Phys. Rev. Lett. **61**, 165 (1988).
[19] P. Martin, V. Veniard, A. Maquet, P. Francken, and C. J. Joachain, Phys. Rev A **39**, 6178 (1989).
[20] P. Francken, Y. Attaourti, and C. J. Joachain, Phys. Rev. A **38**, 1785 (1988).
[21] I. I. Sobelman, *Introduction to the Theory of Atomic Spectra* (Pergamon, New York, 1972), p 272.
[22] F. W. Byron Jr., P. Fancken, and C. J. Joachain, J. Phys B **20**, 5487 (1987).
[23] A. Cionga, F. Ehlotzky, and G. Zloh, Phys. Rev. A **64**, 043401 (2001).
[24] B. H. Bransden and C. J. Joachain, *Physics of Atoms and Molecules*, 2nd ed. (Pearson Education).
[25] A. Chattopadhyay and C. Sinha, Phys. Rev A **72**, 053406 (2005).
[26] M. Brauner, J. S. Briggs, and H. Klar, J. Phys. B **22**, 2265 (1989).
[27] . G. N. Watson, *A Treatise on the Theory of Bessel Functions*, 2nd ed. (Cambridge University Press, Cambridge, UK, 1944).
[28] G. Ferrante, C. Leone, and F. Trombetta, J. Phys. B **15**, L475 (1982).
[29] S. Ghosh Deb, S. Roy, and C. Sinha, Eur. Phys. J. D **55**, 591 (2009).